

PAPER • OPEN ACCESS

SEM investigation of the microstructure of cast CuNiAlCoFe equiatomic high entropy alloy

To cite this article: O A Chikova *et al* 2019 *IOP Conf. Ser.: Mater. Sci. Eng.* **699** 012007

View the [article online](#) for updates and enhancements.

INTERNATIONAL OPEN ACCESS WEEK
OCTOBER 19-26, 2020

ALL ECS ARTICLES. ALL FREE. ALL WEEK.
www.ecsdl.org

**NOW
AVAILABLE**

SEM investigation of the microstructure of cast CuNiAlCoFe equiatomic high entropy alloy

O A Chikova^{1,2}, D S Chezganov¹, V S Tsepelev¹ and V Yu Ilyin¹

¹Ural Federal University, 620002 Ekaterinburg, Russia

²Ural State Pedagogical University, 620017 Ekaterinburg, Russia

O.A.Chikova@urfu.ru

Abstract. Microheterogeneity and crystallization conditions of the equiatomic high-entropy CuNiAlCoFe alloy were studied by measuring the viscosity during heating/cooling, as well as visualizing the microstructure after solidification. The CuNiAlCoFe liquid alloy showed different temperature dependences of viscosity upon heating to 2070 K and subsequent cooling. Since the coinciding part of the temperature dependences was absent, complete destruction of the microheterogeneity of the melt after heating to 2070 K did not occur. Heating the melt to higher temperatures was not possible due to the evaporation of the metal. The melt viscosity during cooling is higher than that during heating; this is observed when microheterogeneity is dispersed. The CuNiAlCoFe alloy obtained as a result of the experiment at a crystallization rate of 10 K/s had a typical microstructure of cast dendrite. Dendrites consisted of a eutectic (α -Al + CuAl₂+Cu₄NiAl₇) and included primary crystals of CoCu₂Al₇ and FeCu₂Al₇. The interdendritic space contained small Cu₄NiAl₇ crystals.

1. Introduction

High entropy alloys (HEAs) CuNiAlCoFe have a combination of excellent magnetic and mechanical properties [1]. High-entropy alloys are an object of advanced extensive structural research; however, the properties of the liquid state and process features of liquid phase separation of these materials, which are relevant to their production, have been far less explored. In this work, the liquid phase separation in equiatomic alloys of CuNiAlCoFe has been qualitatively studied based on the theory of absolute reaction rate by measuring the viscosity during the heating/cooling process, as well as by imaging of microstructure after solidification.

The properties of highly entropic equiatomic alloys CuNiAlCoFe in the liquid state and the conditions for their crystallization were not studied previously. The alloys of AlCoCrCuFeNi and AlCoCuFe only were studied in a wide temperature range. It was found that a negative excess volume of the Al-containing liquid alloys correlated with a negative enthalpy of the mixture and the change of the excess volume was affected by two basic effects, namely, compression of the Al matrix and formation of compounds in the melt [2].

The separation of the liquid phase in the highly entropic CoCrCuFeNi alloy was studied. Liquid phase separation occurred upon supercooling equal to or exceeding 100 K [3]. The effect of the phase composition on the magnetic and mechanical properties of high-entropy alloys (HEA) FeCoNi(CuAl)_x ($x = 0-1.2$, in molar ratios) was studied. The crystal structure of FeCoNi(CuAl)_x HEAs transformed from single face-centred cubic (FCC) phase for $0 \leq x \leq 0.6$ to body-centred cubic (BCC) phase combined with minor FCC phase for $0.9 \leq x \leq 1.2$, whereas FCC plus BCC duplex phases were found in the range



of $0.7 \leq x < 0.9$. Transmission electron microscopy images of $\text{FeCoNi}(\text{CuAl})_{0.8}$ alloy showed large number of FCC Cu-rich nano-precipitates dispersed in the BCC matrix [1]. The alloys CuNiAlCoFe had a typical cast dendrite microstructure consisting of a dominated BCC and FCC solid solution [4].

2. Experimental

The samples CuNiAlCoFe alloy of equiatomic composition were obtained by vacuum arc melting at laboratory. High purity metals of aluminium (purity 99.9%), copper of the Mk00 brand (purity 99.98%) and carbonyl iron (purity 99.98%) were used as initial components.

The kinematic viscosity was measured by the oscillating cylinder method during heating and subsequent cooling. The measurements were carried out in the temperature range of liquidus up to 2070 K with the isothermal delay no less than 30 min at relatively small (50 K) step wise temperature changes. The temperature was maintained with precision of 1 K using a high-precision controller. The vibration parameters were measured by an optical method using a system of vibration photo recording. The BeO crucibles were used in all experiments. The experiments were carried out in a high-purity helium atmosphere at a pressure of 10^5 Pa. The systematic error of measuring viscosity was 3% and including the random error was not greater than 1.5% at the confidence level of 95%.

Metallographic investigation of the structure of the alloys was carried out by conventional methods. The cooling rate during the crystallization of the samples for metallographic investigation was 10 K/s. The surface microstructure was studied by stereo optical microscopy using Neophot32 (Carl Zeiss, Germany) after electro-polishing. The optical microscopy study was carried out for the samples after etching (alcoholic solution of 3% HNO_3) and without etching. The microhardness testers PMT-3 at applied load of 2 N (measuring error 5%) were used for measuring the mechanical properties. The values of microhardness were averaged on the basis of ten measurements. A metallographic study was carried out on a scanning electron microscope (SEM). The surface chemical elemental distribution was measured by energy-dispersive X-ray spectroscopy (EDS) using SEM Merlin (Carl Zeiss, Germany) equipped with X-Max^NX-ray spectrometer (Oxford Instruments, UK). The data were acquired and analysed by Aztec software (Oxford Instruments, UK). The SEM was used for visualization of surface morphology and structural defects in secondary electron mode with the resolution down to 2 nm. The EDS was applied for revealing the elemental composition of defects and inclusions.

3. Results and discussion

Figure 1 presents the results of a viscosimetric study of CuNiAlCoFe liquid alloy with equiatomic composition. This melt demonstrates hysteresis-like viscosity temperature dependence for heating/cooling cycle. The coinciding parts of the temperature dependences of the viscosity, obtained by heating and cooling, are absent. This means that the transition of the melt to a state of true solution after heating up to 2070 K at complete destruction of the microheterogeneity did not occur. The viscosity changes occur nonmonotonically during heating. The significant increase in the viscosity during cooling at low temperatures (near liquidus) is shown. The increase of melt viscosity can explain the dispersing of microinhomogeneities at non-complete destruction of the microheterogeneity [5]. The microheterogeneity of CuNiAlCoFe liquid alloys is understood as the presence of dispersed particles, which are enriched in Fe, Co, Al, Ni, Cu and separated by an interfacial surface from the rest of the melt.

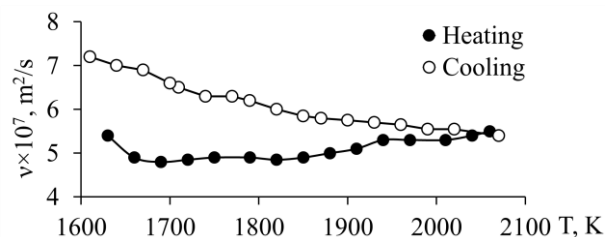


Figure 1. The temperature dependences of the kinematic viscosity of the CuNiAlCoFe melts.

The temperature dependency of viscosity for cooling is monotonic and obeys an Arrhenius law [5]:

$$\nu = A \exp\left(\frac{E}{RT}\right) \quad (1)$$

Our attention was focused on the changing characteristics of the viscous flow of the CuNiAlCoFe melt: the activation energy of viscous flow E and the entropy factor A in the Arrhenius equation.

According to the theory of absolute reaction rate [6], melt viscosity can be described by the equation:

$$\nu = \frac{hN_A}{\mu} \exp\left(\frac{\Delta G^\ddagger}{RT}\right) = \frac{hN_A}{\mu} \exp\left(-\frac{\Delta S^\ddagger}{R}\right) \exp\left(\frac{\Delta H^\ddagger}{RT}\right) \quad (2)$$

where h - Planck's constant, N_A - Avogadro constant, ΔG^\ddagger - the free activation energy of viscous flow, μ - the molar mass, ΔH^\ddagger - the enthalpy of viscous flow activation, ΔS^\ddagger - the entropy of viscous flow activation, R - the universal gas constant and T - temperature (K). The Entropy factor in the Arrhenius equation depends on the entropy of the viscous flow ΔS^\ddagger :

$$A = \frac{hN_A}{\mu} \exp\left(-\frac{\Delta S^\ddagger}{R}\right) \quad (3)$$

We calculated the activation energy $E = 27.29 \text{ kJ} \cdot \text{mol}^{-1} \text{K}^{-1}$ and the entropy of activation $\Delta S^\ddagger = -21.48 \text{ J} \cdot \text{K}^{-1}$ of viscous flow upon cooling.

We carried out the metallographic study of the microstructure of the ingots obtained after the viscosity measurement. Images of microstructure of samples are shown in Figures 2 and 3.

The microstructure of ingots is homogeneous over the cross section and consists of dendrites and the interdendritic layers of multi-phase composition. The multiple phases in the dendrites and the interdendritic space were distinguished by optical microscopy after chemical etching. The different of phases show sharply a differ in microhardness HV (MPa). According to data on microhardness, we conclude about complex phase composition of dendrites and interdendritic space. For example, microhardness from the periphery to the centre of the dendrite changes the value: 2834-3050 MPa. In the interdendritic space, inclusions having microhardness of 3511, 2187, and 2932 MPa were found.

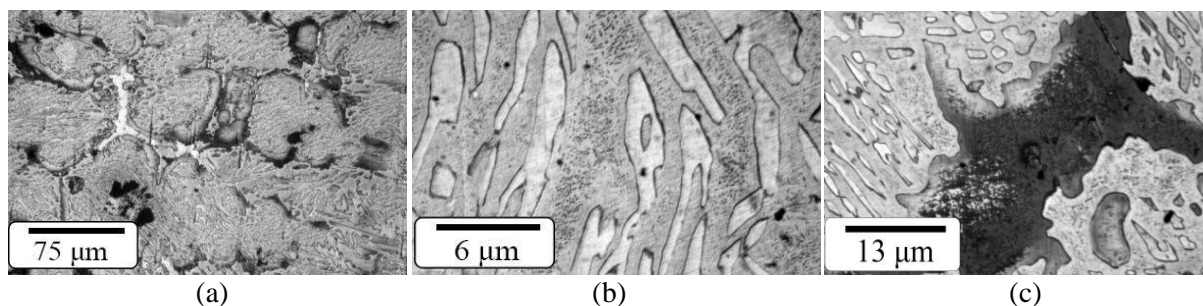


Figure 2. The microstructure of CuNiAlCoFe alloy ingots (optical microscopy): (a) dendrites, (b) intrinsic microstructure of dendrites, (c) interdendritic space.

Table 1. Elemental composition of CuNiAlCoFe alloy at the points marked at Figure 3.

	C	Al	Cu	Fe	Co	Ni
Spectrum 1, wt. %	4.68	6.78	33.73	17.73	17.84	19.24
Spectrum 2, wt. %	4.60	12.15	22.85	16.86	20.30	23.24

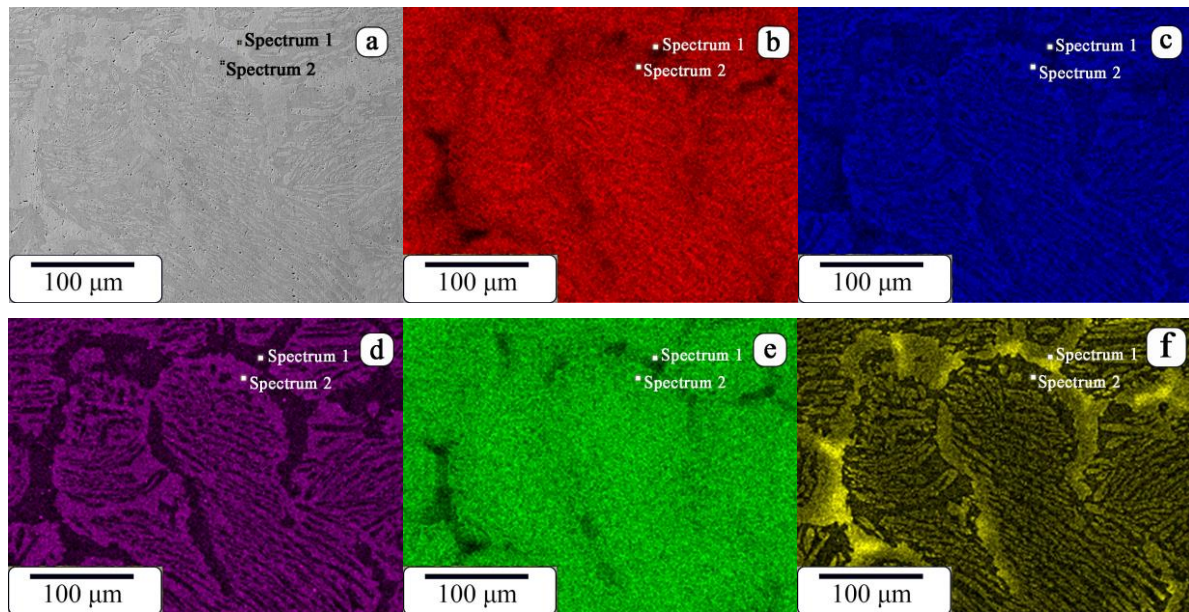


Figure 3. (a) SEM image of surface microstructure of CuNiAlCoFe alloy ingots. Elemental distributions: (b) Fe, (c) Ni, (d) Co, (e) Al, (f) Cu.

The dendrites consist of ternary eutectic (α -Al + CuAl_2 + Cu_4NiAl_7) and large primary crystals of CoCu_2Al_7 and FeCu_2Al_7 isomorphous compounds [1,3,4,7-11]. The interdendritic space contains small primary crystals of Cu_4NiAl_7 . A significant interdendritic porosity was found. Ab-initio molecular dynamics (AIMD) simulations were used to determine crystal structures of phases at different temperatures in CuNiAlCoFe equiatomic composition [12]. The AIMD results showed a possible coexistence of FCC and BCC phase at the room temperature. The phase diagrams of CuNiAlCoFe system was calculated using a modified thermodynamic approach based on Calculation of Phase Diagrams (CALPHAD) and Muggianu's methods [8-9]. The characterization utilizing SEM, X-ray diffraction, and EBSD confirmed that crystal structures and composition of phases calculated by AIMD and phase diagram simulations.

4. Conclusion

High entropy CuNiAlCoFe (HEA) alloys have a combination of superior magnetic and mechanical properties. Microheterogeneity and crystallization conditions of the equiatomic high-entropy CuNiAlCoFe alloy were qualitatively studied by measuring viscosity based on the theory of absolute reaction rates, as well as visualization of the microstructure after solidification.

The equiatomic liquid alloy CuNiAlCoFe exhibits a hysteresis-like temperature dependence of viscosity upon heating to 2070 K and cooling. The coincident parts of the temperature dependences of viscosity, which are obtained by heating and cooling, are absent. This means that the melt did not undergo the transition to the true solution state after heating to 2070 K, and microheterogeneity remained. An increase in the melt viscosity during cooling can explain the process of microheterogeneity dispersion. A significant increase in viscosity at low temperatures (near liquidus) during cooling is characteristic.

The CuNiAlCoFe alloys demonstrated a typical cast dendrite microstructure consisting of dominated body-centred-cubic and the face-centred-cubic solid solutions. The dendrites consist of eutectic (α -Al + CuAl_2 + Cu_4NiAl_7) and include the primary crystals of CoCu_2Al_7 and FeCu_2Al_7 . The interdendritic space contains small primary crystals of Cu_4NiAl_7 . A significant interdendritic porosity was found.

Acknowledgements

The equipment of the Ural Centre for Shared Use “Modern nanotechnology” UrFU was used. Authors are grateful for the support of experimental works by Act 211 Government Russian Federation, contract № 02.A03.21.0006.

References

- [1] Zhang Q, Xu H, Tan XH, Hou XL, Wu S W, Tan G S and Yu L Y 2017 *J. Alloys Compd.* **693** 1061-7
- [2] Plevachuk Y, Brillo J and Yakymovych A 2018 *Metall. Mater. Trans. A* **49** 6544-52
- [3] Guo T, Li J, Wang J, Wang Y, Kou H and Niu S 2017 *Intermetallics* **86** 110-5
- [4] Zhuang Y X, Liu W J, Chen Z Y, Xue H D and He J C 2012 *Mat. Sci. Eng. A* **556** 395-9
- [5] Chikova O A, Sinitsin N I and V'yukhin V V 2019 *Russ. J. Phys. Chem. A* **93** 1435-42
- [6] Chikova O A, Tsepelev V S and Moskovskikh O P 2017 *Russ. J. Phys. Chem. A* **91** 979-83
- [7] Raghavan V 2006 *J. Phase Equilib. Diff.* **56** 389-91
- [8] Kundin J, Wang P, Emmerich H and Schmid-Fetzer R 2014 *Eur. Phys. J. Spec. Top.* **223** 567-90
- [9] Wang C-H, Chen S-W, Chang C-H and Wu J-C 2003 *Metall. Mater. Trans. A* **34** 199-209
- [10] Yadav T P, Shaz M A, Tiwari R S and Srivastava O N 2003 *Zeitschrift fur Kristallographie* **218** 12-6
- [11] Yadav T P, Mukhopadhyay N K, Tiwari R S and Srivastava O N 2007 *Mat. Sci. Eng. A* **448-451** 1052-6
- [12] Kivy M, Beyramali Z, Asle M and Lekakh S 2017 *Mater. Des.* **127** 224-32